Accepted Manuscript

Analysis of the dynamic air conditioning loads, fuel consumption and emissions of heavy-duty trucks with different glazing and paint optical properties

Analysis of the dynamic air conditioning loads, fuel consumption and emissions of heavy-duty trucks with different glazing and paint optical properties

João P. Vale[a], Pedro G. Alves[a], Soraia F. Neves[a], Lars Nybo[b], Andreas D. Flouris[c], Tiago S. Mayor[a,*]

[a] *SIMTECH Laboratory, Transport Phenomena Research Centre, Engineering Faculty of Porto University, Rua Dr. Roberto Frias, 4200-465 Porto, Portugal*

[b] *Department of Nutrition, Exercise and Sports, University of Copenhagen, 2100 Copenhagen, Denmark*

[c] *FAME Laboratory, Department of Exercise Science, University of Thessaly, Trikala 42100, Greece*

[*] Corresponding author: tiago.sottomayor@fe.up.pt (Tiago S. Mayor)

Analysis of the dynamic air conditioning loads, fuel consumption and emissions of heavy-duty trucks with different glazing and paint optical properties

The European transportation sector employs 10 million people and accounts for 4.6 % of the European Union GDP. Due to climate change, this workforce is increasingly affected by high temperatures and radiant loads, particularly during summer. They rely on air conditioning (AC) to minimize heat inside the truck cabins, increasing fuel consumption and tailpipe emissions. Because sustainable transportation is crucial for climate change mitigation, we developed a numerical investigation on the dynamic thermal exchanges of cabins of heavy-duty trucks in realistic conditions of a summer workday, to quantify the potential impact of interventions in the glazing and paint optical properties, over the truck AC loads. We observed that the changes in air temperature and solar irradiation throughout the workday imply substantial variations in the truck's AC loads and, consequently, in its fuel consumption and tailpipe emissions. Furthermore, windshields and side windows with transmissivity of 0.33 instead of typical 0.79 and 0.84, respectively, can reduce AC loads by up to 16 %. External paints with reflectivity of 0.70 instead of 0.04 can reduce the AC loads by up to 30 %, whereas cumulative changes to glazing and paint can reduce the AC load by up to 40 %. These interventions can lower fuel consumption and emissions by up to 0.4 %. These results show that important improvements in fuel efficiency and tailpipe emissions are possible, if the research community, policy makers and industry stakeholders successfully promote the adaptation of the European transportation fleet.

Keywords: heavy-duty trucks; air conditioning loads; optical properties; fuel consumption; tailpipe emissions.

Word count: 9878

Introduction

Thermal comfort is of paramount importance for humans. To maintain an adequate body core temperature, our thermoregulatory system must counteract the effects of the environment (Parsons 2003). With climate changes becoming more evident, events with

higher-than-normal temperatures are increasing in frequency and intensity (Watts et al. 2015). This is increasingly challenging from a thermoregulatory perspective, especially when the exposure is long (Hajat, O'Connor, and Kosatsky 2010). Heavy-duty vehicle operators, such as truck or bus drivers, experience often thermally challenging environments during a typical summer workday (Venugopal et al. 2015), over which they are exposed to high thermal loads during long periods. This can lead to heat strain and heat-related illness (including heat exhaustion and heat stroke), decreased productivity and increased likelihood of work accidents (Brotherhood 2008; Flouris et al. 2018; Hanna et al. 2011).

Prolonged exposure to solar radiation and high external air temperature are some of the causes of heat stress inside a vehicle (Dadour et al. 2010). In such scenario, the air-conditioning (AC) is used to compensate for the increased loads in the cabin so that its internal temperature is maintained within a comfortable range. However, the AC usage decreases fuel efficiency and increases tailpipe emissions (Walgama et al. 2006). Therefore, it is of great importance to minimize the thermal loads affecting the vehicle cabin, and thus the need for high cooling loads (i.e., AC).

Studies of the thermal loads affecting vehicle cabins have been done using distinct approaches. Zheng et al. (Zheng, Mark, and Youmans 2011) developed a one-step calculation method to estimate vehicle heat loads. Their wind-tunnel experiments indicated that their thermal load predictions had a relative error below 8 % despite being based on a simple mathematical model. John et al. (John et al. 2013) used an approach based on computational fluid dynamics to identify the optimal combination of open windows to increase ventilation inside a bus. Fujita et al. (Fujita et al. 2001) developed a method that coupled heat balance equations and simulations based on computational fluid dynamics for a typical vehicle. They were able to predict the car thermal

environment for different scenarios of air temperature, solar radiation, ventilation rate and air conditioning settings.

Both experimental and numerical methods have been used to study the effects of vehicle properties on thermal loads and AC usage. Lahimer et al. (Lahimer et al. 2018) studied experimentally the effect of solar reflective covers on the air temperature of a vehicle and found that aluminum covers on the glazing and roof reduced the air temperature inside a parked car by up to 17 °C. Li and Sun (Li and Sun 2013) performed numerical simulations to investigate how environmental and design variables affect the thermal loads inside train or metro passenger compartments. They found that fresh air volume, room design temperature and passenger load have a significant impact on the heat loads. Mezrhab and Bouzidi (Mezrhab and Bouzidi 2006) studied the thermal comfort inside a car cabin in summer. They reported that reflective glazing and white colored paint can decrease the temperature inside a car parked under the sun by 10 °C and 7 °C, respectively. A study by Rugh et al. (J. P. Rugh et al. 2007) reports a reduction of 25 % in the fuel consumed to power the AC when the vehicle is equipped with solar-reflective paint and glazing. Levinson et al. (Levinson et al. 2011) demonstrated that reducing the car shell reflectivity by 0.5 can lower the soak air temperature by 5-6 °C. The same authors also report that a white or silver colored car may have its fuel consumption reduced by 0.21 L/100 km (1.9 %) and CO_2 emissions by 4.9 g/km (1.9 %), compared to the same vehicle colored in black.

Despite the interesting contributions mentioned above, extrapolating their results for other types of vehicles, namely heavy-duty trucks, is not straightforward because of several aspects affecting the cabin thermal exchanges with the environment: (1) car and heavy-duty trucks have very different geometry and glazing to shell surface areas ratios, which changes the balance between the different loads to be compensated for by the AC

systems, and (2) the typical pattern of utilization of both vehicles is very different, with the latter implying longer trips with less frequent changes in direction. Furthermore, a portion of the relevant literature is focused on parked or stationary vehicles (Horak et al. 2017; Torregrosa-Jaime et al. 2015; Kilic and Sevilgen 2009; Akyol and Kilic 2010; Orzechowski and Skrobacki 2016), which implies load variations over time that are different from those of moving vehicles. In addition, the environmental conditions used in most of these studies are constant throughout the experiments/simulations, which is not an accurate representation of the variation in solar irradiation and air temperature throughout a typical day. Also, while the overall effect of the glazing and paint optical properties on the heat loads affecting a vehicle is known (Gravelle, Robinson, and Picarelli 2015; Pokorny, Fiser, and Jicha 2014; J. P. Rugh, Hendricks, and Koram 2001; R. B. Farrington et al. 1998b; Olson et al. 2014), the chosen properties are often not directly associated with existing materials/products in the market, which may decrease the applicability of some of the findings to real situations. Therefore, analyzing the time-dependent variations in heat loads throughout a day for heavy-duty trucks with different glazing and paint optical properties (based on existing products in the market), and the resulting change in AC loads, fuel consumption and tailpipe emissions, would improve our knowledge of the real environmental and economic benefit of these modifications.

Finally, there are open-source tools (e.g. VECTO, ADVISOR) to predict the fuel consumption of different vehicles. However, they are focused on the effect of vehicle components and driving strategy, rather than on the effect of the thermal environment over the air conditioning loads. The AC cooling loads as well as other auxiliary loads are often considered constant, which is not the case in real scenarios. This was corroborated by the results of a questionnaire on VECTO's capabilities, in which most

respondents considered the auxiliary load / energy management of this tool as "insufficiently captured" (Joint Research Centre 2016). While recent updates to VECTO have been implemented to better represent real-world driving conditions (Rexeis et al. 2019), these changes do not consider the influence of the AC efficiency and the paint and glazing reflectivity which were identified as relevant in the 2016 Join Research Centre questionnaire, nor the influence of the dynamic heat loads affecting the truck cabin throughout the day, and their impact on the AC cooling power. For buses and coaches, VECTO has an auxiliary module to predict the auxiliary loads based on AC compressor type, bus cabin size and passenger number (Zacharof et al. 2019). However, this module still considers an AC load that is constant over time. Therefore, there is a need for a tool allowing the prediction of the AC cooling loads for different and dynamic thermal environments, to enable a more detailed quantification of the impact of the AC on the fuel consumption and tailpipe emissions of heavy-duty trucks.

Against this background, we have developed a numerical investigation on the dynamic thermal loads affecting the cabins of moving heavy-duty trucks during a typical summer day, considering exposure to realistic environmental conditions (e.g. ambient temperature and solar loads varying over time). With the goal of assessing the possibility of decreasing the required AC loads and, consequently, the fuel consumption and associated emissions, we investigated the impact of changes in the optical properties of the glazing and paint cabin components, over the AC loads required to maintain a constant cabin temperature throughout a workday. For greater representativeness of the findings, all parameters considered in the analysis were based on materials/products currently existing in the market.

Material and methods

Physical situation under consideration

In Europe, most heavy-duty trucks are of cab-over-engine type (Martini, Gullberg, and Lofdahl 2018). For that reason, the dimensions of the virtual truck considered in the present study (Table 1) were adapted from the Volvo specifications for cab-over-engine trucks (Volvo, n.d.). The chosen cabin dimensions are representative of the typical average-size cab-over-engine truck as they do not significantly differ from those of other truck manufactures (MAN n.d.; Mercedes Benz n.d.). The virtual cabin has nine surfaces: roof, back, base, front, windshield, right and left doors and side windows. The windshield and side windows are made of glass, and the cabin body surfaces were assumed to be made from a combination of 1 mm of steel, 10 mm of insulation and 1 mm of lining (Morello et al. 2011; Khayyam et al. 2011; Marcos et al. 2014; Akyol and Kilic 2010). The properties of the glass and the cabin body surfaces are shown in Table 1.

TABLE 1 IS LOCATED HERE

The virtual truck was assumed to be exposed to the summer conditions in Évora, Portugal (38.70° N, 7.78° W), which is a good representation of the warm/hot summer in the southern European countries (Figure 1). The virtual truck was assumed to be heading either south or west, at 80 km/h, with an average air velocity inside the cabin of 0.5 m/s (Musat and Helerea 2009; Kilic and Sevilgen 2009). Simulations were performed for a work period between 8 AM to 7 PM, to capture the variation of the thermal loads during the daytime period where heat and solar radiation are most prevalent.

FIGURE 1 IS LOCATED HERE

Because multi-manning (also known as team driving) is considered a safe and efficient operating procedure for heavy-duty trucks (Kopfer and Buscher 2015; Klauer et al. 2003), a driver and a passenger were assumed to be seated inside the cabin, with the dimensions and metabolic rates shown in Table 2.The hourly ambient temperatures over time were retrieved from the EnergyPlus database("EnergyPlus - Evora, Portugal - Weather Data" n.d.) for the 21st of July, which were fitted by a 3rd order polynomial to enable temperature predictions every 60 s ("EnergyPlus - Evora, Portugal - Weather Data" n.d.) (Figure 1). The relative humidity retrieved from Weather Underground database ("Beja Air Base, Portugal - Weather Underground" n.d.) indicated that a constant humidity of 40 % was a reasonable approximation. The position of the sun at every instant was calculated based on the equations from National Oceanic and Atmospheric Administration ("National Oceanic and Atmospheric Administration" 2021) for the latitude and longitude of Évora, Portugal.

TABLE 2 IS LOCATED HERE

Mathematical model

A lumped element model was used to describe the heat transfer in a truck cabin system, in line with previous works (Fayazbakhsh and Bahrami 2013; Huang et al. 2007; Torregrosa-Jaime et al. 2015; Marcos et al. 2014). Following a heat balance method, the total load affecting the truck cabin ($\dot{Q}_{Tot}$) can be obtained as the sum of the different loads represented in Figure 2a.

$$\dot{Q}_{Tot} = \dot{Q}_{Met} + \dot{Q}_{Dir} + \dot{Q}_{Diff} + \dot{Q}_{Amb} + \dot{Q}_{Vent} + \dot{Q}_{AC} \quad (1)$$

where $\dot{Q}_{Met}$ [W] is the metabolic load associated with the cabin occupants, $\dot{Q}_{Dir}$ [W]

and $\dot{Q}_{Diff}$ [W] are, respectively, the direct and diffuse radiation loads, $\dot{Q}_{Amb}$ [W] is the ambient load, $\dot{Q}_{Vent}$ [W] is the ventilation load and $\dot{Q}_{AC}$ [W] is the cooling load imposed by the air conditioning. The reflected radiation and engine loads were not considered as they are often much smaller than the other loads (Fayazbakhsh and Bahrami 2013; Khayyam et al. 2011). Because the loads in equation (1) vary over time, they were calculated at every time step, assuming quasi-steady-state (i.e. thermal equilibrium in each step).

FIGURE 2 IS LOCATED HERE

Metabolic load

The human body generates heat through its metabolic activity, even at rest (Havenith, Holmér, and Parsons 2002). The heat generated by the driver and passengers is then transferred to the cabin environment. The metabolic load is the sum of the metabolic loads associated to each of the *N* occupants

$$\dot{Q}_{Met} = \sum_{n=1}^{N} M_{q,n} A_{Du} \qquad (2)$$

where M_q [W/m^2] is the rate of metabolic heat production and A_{Du} [m^2] is the DuBois body surface area.

Radiation load

The short-wave solar radiation plays a significant role in the heat gain by vehicle cabins exposed to solar radiation. It is generally divided in the direct, diffuse and reflected components (ASHRAE 1997). Since the reflected radiation is generally negligible compared to the other components, the total radiation load was calculated by

$$\dot{Q}_{Rad} = \dot{Q}_{Dir} + \dot{Q}_{Diff} \qquad (3)$$

The direct radiation is the portion of the solar radiation that irradiates the vehicle directly. It can be calculated by

$$\dot{Q}_{Dir} = \sum_{s=1}^{9} A_s \tau_s \dot{I}_{Dir} \cos\theta_s \qquad (4)$$

For a given external surface s, A_s [m^2] is the surface area, τ_s is the solar transmissivity, and $\dot{I}_{Dir}$ [W/m^2] is the solar irradiance at an angle θ (i.e. the angle between the surface normal and the line connecting the surface and the sun, Figure 2b). The solar irradiance can be calculated using the apparent solar constant (A) and the atmospheric extinction coefficient (B) which are tabulated for each month (ASHRAE 1997) (Table 3)

$$\dot{I}_{Dir} = Ae^{-\frac{B}{\sin\beta}} \qquad (5)$$

where β is the solar altitude angle, calculated based on the vehicle and solar positions (Figure 2b). This solar radiation model is valid for clear days (Wong and Chow 2001), so for other meteorological conditions, a correction parameter should be used to account for the effect of clouds, dust, etc.

TABLE 3 IS LOCATED HERE

The diffuse radiation load $\dot{Q}_{Diff}$ [W/m^2] accounts for the radiation scattered by the atmosphere, and can be obtained by

$$\dot{Q}_{Diff} = \sum_{s=1}^{9} A_s \tau_s \dot{I}_{Diff,s} \qquad (6)$$

where $\dot{I}_{Diff,s}$ [W/m^2] is the intensity of the diffuse radiation. It is calculated by

$$\dot{I}_{Diff,s} = C\dot{I}_{Dir}\frac{1+\cos\Sigma_s}{2} \qquad (7)$$

where C is the sky diffuse factor, tabulated for each month (ASHRAE 1997), and Σ_s is

the tilt angle of the surface s, from the reference horizontal surface. This angle is equal to 90˚ minus the angle between the normal vector n̂ and the reference horizontal surface (Figure 2b).

A portion of the incident radiation is absorbed by the vehicle surfaces, increasing their temperature. There is also emission of long-wave radiation, which can be calculated for each surface according to the Stefan-Boltzmann equation (Boltzmann 1884). The net radiation load on each surface can thus be obtained as the balance between the absorbed and emitted components:

$$\dot{Q}_{Rad,s} = A_s \alpha_s \left(\dot{I}_{Dir} \cos\theta_s + \dot{I}_{Diff,s}\right) - A_s \varepsilon_s \sigma \left(T_s^4 - T_{sky}^4\right) \quad (8)$$

where α_s is the surface absorptivity, ε_s is the surface emissivity, σ is the Stefan-Boltzmann constant (5.67×10^{-8} W/(m^2·K^4)), T_s [K] and T_{sky} [K] are respectively the surface and sky temperatures. The base of the truck is parallel to the road, thus, we assumed that its external surface does not absorb direct or diffuse solar radiation, nor does it emit long-wave radiation to the sky. The sky temperature can be estimated as a function of the air temperature T_{amb} [K] by (Swinbank 1963)

$$T_{sky} = 0.0552\, {T_{amb}}^{1.5} \quad (9)$$

Ambient load

The ambient load $\dot{Q}_{Amb}$ [W] represents the heat transferred by conduction through the cabin shell/surfaces. It can be calculated by:

$$\dot{Q}_{Amb} = \sum_{s=1}^{9} A_s U_s (T_s - T_i) \quad (10)$$

where U_s [W·m^{-2}·K^{-1}] is the overall heat transfer coefficient, i.e.

$$U_s = \frac{1}{R_s} \text{ where } R_s = \frac{1}{h_o} + \frac{\delta_s}{k_s} + \frac{1}{h_i} \qquad (11)$$

Here, δ_s [m] is the material thickness, k_s [W·m^{-1}·K^{-1}]is the material thermal conductivity, and h_0 and h_i [W·m^{-2}·K^{-1}] are the external and internal convection coefficients, respectively. These can be estimated based on the air velocity V [m/s] by

$$h = 0.6 + 6.64\sqrt{V} \qquad (12)$$

The net ambient load $\dot{Q}_{Amb,s}$ [W] absorbed by each surface was then calculated as the difference between the heat gained from the ambient and the heat released to the cabin.

$$\dot{Q}_{Amb,s} = A_s U_s (T_{amb} - T_s) - A_s U_s (T_s - T_i) = A_s U_s (T_{amb} - 2T_s + T_i) \qquad (13)$$

where T_{amb}, T_s and T_i [K] are the environment, surface, and cabin temperatures, respectively.

Ventilation load

The passengers breathing causes the CO_2 concentration to increase over time and so, a supply of fresh air must be ensured. Because of this, the cabin pressure is usually slightly higher than the ambient pressure, which causes air leakage from the cabin to the outside at a certain flow rate.

In this work we assume that the mentioned pressure difference is constant and that, in steady-state, the flow rate of air entering the cabin at the external temperature and relative humidity, is equal to the flow rate of the air leaving the cabin at its temperature and relative humidity. Based on previous literature (Fayazbakhsh and Bahrami 2013; R. B. Farrington et al. 1998a; Lahimer et al. 2018), we considered a ventilation flow rate of 0.01 m^3/s.

The ventilation load $\dot{Q}_{Ven}$ [W] is directly related to the air exchanged between the ambient and the cabin, and thus has latent and sensible components. It can be calculated based on the ventilation flow rate and the ambient and cabin enthalpies by

$$\dot{Q}_{Ven} = \dot{m}_{ven}(e_o - e_i) \quad (14)$$

where $\dot{m}_{ven}$ [kg/s] is the ventilation mass flow rate, and e_o and e_i [J/kg] are the ambient and cabin enthalpies, respectively. The enthalpies were calculated by

$$e = 1006 \cdot T + \mathrm{X} \cdot (2.501 \times 10^6 + 1770 \cdot T) \quad (15)$$

where T [°C] is the ambient or cabin air temperature and X is the humidity ratio

$$X = 0.62198 \frac{\phi P_s}{P - \phi P_s} \quad (16)$$

Here, φ is the relative humidity [%], P [Pa] is the air pressure and P_s [Pa] is the water saturation pressure at the air temperature T.

Cooling load

The air conditioning (AC) is tasked with compensating for the effect of the loads affecting the cabin, to maintain the cabin temperature within a comfortable range. Its cooling load $\dot{Q}_{AC}$ was calculated considering the several different thermal loads described above:

$$\dot{Q}_{AC} = -\left(\dot{Q}_{Met} + \dot{Q}_{Dir} + \dot{Q}_{Diff} + \dot{Q}_{Amb} + \dot{Q}_{Vent}\right) - \frac{\ln|T_0 - T_{comf}| \cdot (DTM + m_a c_a)(T_i - T_{comf})}{t_p} \quad (17)$$

where T_{comf} [K] is the required comfort temperature in the cabin, T_0 [K] is the initial cabin temperature, DTM [J/K] is the cabin deep thermal mass, m_a [kg] and c_a [J·kg^{-1}·K^{-}

[1]] are the cabin air mass and air specific heat respectively, and t_p [s] is the pull-down time. The latter is the time needed for the cabin to reach the comfort temperature starting from the initial condition.

We assumed a deep thermal mass of 10800 J/K, by estimating the heat capacity of the cabin insulation and seats (details of this research data can be found elsewhere (Vale, Alves, and Mayor 2020)). Following ASHRAE comfort standards for summer (ASHRAE 1997), the comfort temperature and relative humidity inside the cabin were set to 23 °C and 50 %, respectively. The pull-down time to achieve the comfort temperature was assumed to be 600 s (10 min).

Calculation procedure

The loads affecting the cabin were calculated during the entire simulation period, at each time-step (Δt [s]), after which the change in temperature of the cabin air (ΔT_i [K]) and the cabin surface elements (ΔT_s [K]) could be calculated as

$$\Delta T_i = \frac{\dot{Q}_{Tot}}{DTM + m_a c_a} \Delta t \quad (18)$$

$$\Delta T_s = \frac{\dot{Q}_{Rad,s} + \dot{Q}_{Amb,s}}{m_s c_s} \Delta t \quad (19)$$

where $\dot{Q}_{Tot}$ [W] represents the total load on the cabin (from equation 1), and m_s [kg] and c_s [J·kg^{-1}·K^{-1}] are the mass and specific heat of the material composing the surface s.

Fuel consumption and tailpipe emissions

To estimate fuel consumption, we assumed that a typical AC system has a maximum cooling load (i.e. cooling capacity) of 4.5 kW (Hoke and Greiner 2005; Levinson et al. 2011; Alkan and Hosoz 2010; Qi, Zhao, and Chen 2010; Akyol and Kilic 2010) and a

coefficient of performance (COP) of 2, based on the range found in the literature (Andrew Pon Abraham and Mohanraj 2019; Samuel, Austin, and Morrey 2002; Qi, Zhao, and Chen 2010). This implies a maximum compressor load of 2.25 kW, as the load used to power the AC when it is providing the maximum cooling load can be obtained by dividing the cooling capacity by the coefficient of performance (4.5 kW / 2 = 2.25 kW).

We considered that the auxiliary loads of heavy-duty trucks correspond, on average, to 5.6 kW, and account for 5% of their fuel consumption (Tansini et al. 2019). Based on this relation, an AC system with a maximum compressor load of 2.25 kW increases the fuel consumption by up to 2%. Moreover, we assumed that the fuel consumption linearly increases with the cooling load provided by the AC system (J. P. Rugh, Hendricks, and Koram 2001), up to the mentioned 2%.

We considered that a standard truck has a fuel consumption of 35 L/100 km when not using air conditioning (Volvo 2018; Saari et al. 2016), that the tailpipe emissions vary linearly with the variations in fuel consumption, and that 7 g of NO_x, 0.1 g of particulate matter and 2.6 kg of CO_2 are released per L of consumed fuel (Na et al. 2015; Fontaras et al. 2016; Muncrief and Sharpe 2015; Volvo 2018; Saari et al. 2016). We used these relations to estimate the increase in fuel consumption and tailpipe emissions caused by using the AC system, for realistic environmental conditions and various properties of the cabin materials.

Simulation cases

Because the AC cooling load, the fuel consumption and the tailpipe emissions vary with the loads affecting the cabin, we focused our attention on the elements that can influence the latter, such as the windshield and side windows (as glazing influences the amount of radiation entering the cabin), and the external paint (which affects the portion

of radiation reflected by the shell). Each of these elements represent very different portions of the cabin total external surface (Table 1), and the contributions of the different loads to the net result considered are likely very different. For that reason, it is important to assess the impact of changing the properties of each of the abovementioned cabin elements, both over the loads affecting the cabin, and the cooling load required to maintain the comfort temperature. This was done by considering two sets of optical properties, which allow more and less heat to reach the cabin. These properties were defined based on existing, commercially available products.

TABLE 4 IS LOCATED HERE

Scenario 1 considers a truck with standard properties, i.e. a windshield made of a tinted laminated glass (Mallick 2012), side windows made of tinted monolithic glass (Mallick 2012) and external paint having the average reflectivity ($\rho = 0.32$) of the 180 paints in the "CoolCars" database (Levinson et al. 2010) (Figure 3). Scenario 2 considers a truck with high-transmissivity glazing, i.e. a windshield made of clear laminated glass (Hodder and Parsons 2007) and side windows made of clear monolithic glass (Hodder and Parsons 2007). On the other hand, scenario 3 considers a truck with low-transmissivity glazing, where both windshield and side windows are made of a low-transmissivity glass such as Sungate® (J. Rugh 2009; Levinson et al. 2010). Scenarios 4 and 5 consider trucks with standard glazing (as in scenario 1) and two external paints having different reflectivity, i.e. the minimum ($\rho = 0.04$, scenario 4) and maximum ($\rho = 0.70$, scenario 5) reflectivity values of the "CoolCars" paints database (Levinson et al. 2010), respectively. Scenario 6 considers a truck with high-transmissivity glazing (as in scenario 2) and low-reflectivity paint (as in scenario 4, two modifications that allow more heat to enter the cabin. Lastly, scenario 7 considers a truck with low-

transmissivity glazing (as in scenario 3) and high-reflectivity paint (as in scenario 5), modifications that minimize the heat entering the cabin. The specific optical properties of the materials considered in each scenario are detailed in Table 4.

FIGURE 3 IS LOCATED HERE

Assumptions and numerical computation

Geometrical details of the cabin elements (Table 1), environmental conditions (Figure 1) and initial temperature of surfaces and cabin (25 °C) were required as input. The series of equations described above were solved sequentially using the Euler method, to estimate the different loads affecting the cabin and the changes in temperature of each surface and the air inside the cabin. Calculations were conducted in time-steps of 60 s (found to capture the variation of the different loads over time) for the defined exposure (from 8 AM to 7 PM).

Results and discussion

Model validation

We verified the accuracy in the implementation of the model by comparing its predictions against results by Fayazbakhsh and Bahrami (Fayazbakhsh and Bahrami 2013) regarding the thermal loads affecting a vehicle during a summer afternoon. Using the present model, we replicated the conditions of the mentioned study and compared both results in Figure 4. With the exception of the solar and AC loads, all the other loads obtained with the present model are consistent with those by the Fayazbakhsh and Bahrami (Fayazbakhsh and Bahrami 2013). The slight difference between the obtained direct radiation and AC loads and those in the mentioned work (Fayazbakhsh and Bahrami 2013) is likely due to differences in the radiation parameters considered in the

two studies, since not all radiation parameters are clearly specified in the mentioned study. Furthermore, it may also be due to slight differences in the angles between the sun and the surfaces normal vector, since the vehicle direction (and, subsequently, the normal vectors directions) in the cited work changes randomly around an approximate direction, whereas in the present work we consider a constant vehicle direction equal to the mentioned approximate direction. Within these considerations, the overall consistency between the loads obtained in our work and those in the literature indicate that the model is well implemented and, thus, can be used to investigate the effect of different cabin elements on the cabin thermal loads (including AC).

FIGURE 4 IS LOCATED HERE

In addition to the above verification, we validated the present model by comparing its results with experimental data by Horak et al. (Horak et al. 2017), which measured the cabin temperature of different vehicles idled in multiple environmental conditions. We used the present model to replicate the conditions in the mentioned work and quantified the goodness-of-fit of the predictions by calculating the mean absolute error (MAE, indicative of accuracy and bias), and the root-mean-squared deviation (RMSD, indicative of precision) (Freund and Wilson 2003):

$$MAE = \frac{\sum(x_0 - x_i)}{n} \tag{20}$$

$$RMSD = \sqrt{\frac{\sum(x_0 - x_i)^2}{n}} \tag{21}$$

where x_0 is the actual result (experimental), x_i is the predicted result (numerical) and n is the sample size. Figure 5 shows the comparison between numerical and experimental results after 1h for the different experimental cases. The present model accurately

predicted the cabin temperature after 1h of exposure to environmental conditions, and as such it was considered valid.

FIGURE 5 IS LOCATED HERE

Heat loads inside a truck during a summer workday

We first studied the variation of the thermal loads on the cabin during a typical summer day (Figure 6), for a standard truck (scenario 1) heading south or west.

FIGURE 6 IS LOCATED HERE

As expected, the metabolic load is constant during the exposure period (8 AM to 7 PM) for both directions, as it only depends on the characteristics and number of individuals inside the vehicle. The curves of the direct radiation load (*Q dir*) depend on the vehicle direction, because of the different position of the vehicle surfaces relative to the sun (Figure 6)

For a truck heading south (Figure 6a), radiation enters mostly through the side windows. In the morning, as the solar irradiance increases, so does the direct radiation load entering through the east-facing window. At the solar noon, the direct radiation load decreases slightly, because the sun is positioned almost vertically, which implies an almost null radiation component on the side windows. From that point onward, the west-facing window is irradiated until the sunset. For a truck driving west (Figure 6b), the side windows are mostly unaffected by the solar radiation, since the sun moves from east to west during the day. Because of that, the direct radiation load during the morning and until the solar noon is close to zero, after which it gradually increases as the windshield is irradiated at ever more favourable angles.

The diffuse radiation load (*Q diff*) depends on the solar radiation intensity (equation 8), which varies during the day. Contrary to the direct component, it is not affected by the sun position and is, therefore, not dependent on vehicle direction. For that reason, it increases during the morning and decreases in the afternoon similarly to the solar irradiance (Figure 6).

Heat transfer through convection and conduction through the surfaces is accounted for by the ambient load (*Q amb*). This load varies with the properties of the materials and with the temperatures of the ambient, cabin surfaces and cabin air. The ambient temperature increases throughout the day and starts decreasing mid-afternoon (Figure 1), while the cabin temperature is kept constant by the AC. The external ambient temperature is significantly higher in the afternoon, contributing to the increase in ambient load in that period, compared to the morning.

The ventilation load (*Q vent*) is affected by the ambient and cabin conditions. Although the ambient humidity is considered constant in this work because it does not change significantly ("Beja Air Base, Portugal - Weather Underground" n.d.), the ambient temperature varies throughout the day (Figure 1), and so does the ventilation load (Figure 5a-b). Higher ambient temperature implies that the air entering through leakage and vents is warmer and, thus, contributes to the heating of the cabin.

The cooling load provided by the AC (Q AC) strongly varies during the day and with vehicle direction (Figure 6). The air conditioning system is tasked with compensating for the thermal loads affecting the cabin to maintain its temperature, thus, the higher the thermal loads, the higher the required cooling load.

Finally, the total load (*Q tot*) on the cabin is the sum of all loads including that of the AC. Thus, it is null all the time except at the beginning of the simulation when the cabin temperature is still being corrected by the AC unit. Once the temperature is

corrected, the sum of the loads becomes null and the cabin temperature remains henceforth constant.

The thermal loads are overall higher in the afternoon than in the morning because of the higher ambient temperatures. Trucks heading south and west register different cooling loads along the day, because of the different direct radiation loads affecting them (which depend on the angle of the glazing surfaces relative to the sun). Besides changing with driving direction, the cooling load also varies greatly throughout the day, indicating that performing a dynamic analysis (i.e. time-dependent), instead of a steady-state analysis (i.e. non time-dependent), is crucial to accurately quantify the impact of the environment on the cabin loads. Furthermore, this highlights the importance of considering the cooling load as a variable rather than a constant, when developing vehicle energy management software and strategies.

Glazing and paint modifications

We investigated the effect of changing the glazing and paint optical properties over the thermal loads on the cabin because they influence the cooling load to be provided by the AC unit and, therefore, its energy use. Simulations were run for trucks heading south and west to maximize the solar incidence on the side windows and windshield (south and west directions, respectively; Figure 6). Unless told otherwise, for the sake of representativeness, the results are shown as daily average loads (rather than the peak values occurring around 3 PM when both air temperature and irradiation are high).

Figure 7 shows the daily average thermal loads affecting trucks moving south and west, for the seven different scenarios considered (Table 4). For a standard truck (scenario 1), the ambient load is predominant as it accounts for over 50 % of the thermal loads affecting the cabin (Figure 6). The direct and diffuse radiation loads are also significant, accounting for about 19% of the loads.

Although the variation of the loads throughout the day depends on the vehicle direction (Figure 6), the daily average loads for south and west heading trips differ less than 1% (Figure 7) because the different exposure in the morning and afternoon periods practically cancel out. However, the differences between the loads for other vehicle directions (e.g. north and east, or north and south) may be much larger because of the larger differences in solar exposure for the considered conditions. In addition, the direction may also have an effect on the cabin loads for shorter trips (where there is less cancelling out between morning and afternoon periods) or circular trips (where vehicles may follow two opposite directions in different moments of the day), both of which may require different AC cooling loads depending on the vehicle direction and timing of the trips.

FIGURE 7 IS LOCATED HERE

When modifying the properties of the glazing (scenarios 2 and 3), i.e. by considering high- and low-transmissivity glasses, there were changes mainly in the direct and diffuse loads. The direct radiation loads can be reduced by ≈ 60 % if low-transmissivity glazing (τ = 0.33) is preferred over high-transmissivity glazing (τ = 0.79). This can reduce the total thermal load on the cabin (and thus the cooling load to be provided by the AC) by 16 %. This potential reduction is consistent with the results of Farrington and Rugh (R. Farrington and Rugh 2000), who reported a decrease of 17 % on thermal loads when a Sungate® windshield (τ = 0.33) was used instead of a standard windshield.

We considered low- and high-reflectivity paints (ρ = 0.04 / scenario 4 and ρ = 0.70 / scenario 5, respectively) to investigate the effect of the paint optical properties. As expected, there was a clear reduction in the ambient load when changing from a low-

to a high-reflectivity paint (Figure 7). The higher proportion of radiation reflected when considering a paint with a reflectivity of 0.70 instead of 0.04 implied a reduction in the ambient load of around 50 %. Ultimately, the strong reduction in the ambient load allowed to decrease by 29 % the cooling load required to maintain a constant cabin temperature. This is in line with the results of Lustbader et al. (Olson et al. 2014) who reported a reduction of 21 % on the daily cooling load when using white (ρ = 0.63) instead of black (ρ = 0.05) paint, on parked heavy-duty trucks. In addition, that the paint modification had a much higher impact on the cooling load than that the glazing modification is not surprising, as the external paint influences the heat transfer across a much larger portion of the truck surface area (i.e. 89 % versus 11% for the glazing).

Finally, we investigated the cumulative effect of modifying the glazing and the paint. A warm configuration allowing more heat to enter the cabin was considered in scenario 6 (i.e. high-transmissivity glazing and low-reflectivity paint), whereas a cool configuration allowing less heat to enter the cabin was considered in scenario 7 (i.e. low-transmissivity glazing and high-reflectivity paint). We observed that the daily average cooling load with the cool configuration (scenario 7) is ≈ 41 % lower than that with the warm configuration (scenario 6), due to reductions in the radiation and ambient loads (Figure 7). This is further supported by Figure 8 showing that curve of the radiation and ambient loads ($Q\ dir + Q\ amb$) throughout the day is symmetric to that of the cooling load ($Q\ AC$), for both truck configurations and directions. Furthermore, these curves indicate that the potential reductions in the AC cooling load (via changes in the cabin glazing and pain) are relevant throughout the entire day (and not only at peak conditions, i.e. around 3 PM). These results show that the optimization of the truck cabin glazing and paint optical properties is much more efficent in reducing the energy

used by the AC system than just optimizing each component (glazing or paint) separately.

FIGURE 8 IS LOCATED HERE

Impact on fuel consumption and tailpipe emissions

The changes in the external air temperature and irradiation throughout the day (Figure 1) require variations in the cabin AC loads (Figure 6) and, consequently, in the fuel consumption and tailpipe emissions (Figure 9) of the truck. Accordingly, the consumption and emissions at the warmer period of the day (around 3 PM) are almost 1% higher than those in the colder period (Figure 9). Furthermore, the data in Figure 9 allows to investigate the potential reductions in both the fuel consumption and tailpipe emissions via the warm and cool truck configurations, i.e. scenario 6 (i.e. high-transmissivity glazing and low-reflectivity paint) and scenario 7 (i.e. low-transmissivity glazing and high-reflectivity paint) in Table 4. Considering that the daily average cooling loads required with the warm and cool truck configurations are 2265 W and 1327 W respectively (Figure 6), an AC system with a maximum cooling load (or cooling capacity) of 4.5 kW will have to operate at ≈ 50 % and ≈ 30 % capacity to provide the mentioned cooling loads. This indicates that preferring a cool truck configuration over a warm truck configuration allows to reduce the compressor load by 20 percentage points (from 50 % to 30 %) and the fuel consumption by 0.4 % (i.e. 20 % of the 2 % increase in fuel consumption assumed for an AC operating at maximum cooling load, see section 2.2.7). Furthermore, the tailpipe emissions reduce also by 0.4 %, as they vary linearly with the fuel consumption. These results highlight the importance of carefully choosing the properties of the cabin surfaces, because of the clear potential impacts on the loads affecting the cabin, and the resulting AC loads

needed to compensate them. Glazing elements reducing the amount of radiation entering the cabin and external paints reflecting substantial portions of the solar radiation can enable important reductions in the fuel consumption and emission of pollutants associated with the AC operation throughout the entire workday.

FIGURE 9 IS LOCATED HERE

Conclusion

The use of AC systems to maintain comfortable temperatures inside the cabins of heavy-duty trucks increases fuel consumption and tailpipe emissions. To study how the properties of the cabin surfaces influence the AC loads for realistic environmeantal conditions, a virtual testing environment was developed incorporating the cabin occupants, the cabin materials, and the surrounding environment. Focus was put on the influence of the optical properties of the windshield, side windows and external paint, on the cooling loads required during a summer workday. We considered ranges of optical properties based on existent commercial products and concluded that it is of crucial importance to carefully choose the optical properties of the cabin external surfaces, since savings of up to 40 % could be achieved in the daily average cooling loads, leading to decreases in fuel consumption and emissions of up to 0.4 %. The obtained results highlight the importance of raising awareness about the potential for gains in efficiency and reduction in tailpipe emissions, by the stakeholders of the transportation sector (e.g. vehicle manufacturers, transportation industry, decision makers, regulating bodies, workers unions).

Acknowledgements.

We acknowledge the partial support of the European Union's Horizon 2020 research and innovation programme under grant agreements 668786 (HEAT-SHIELD), 645770 (SmartHELMET), 645710 (ICI-THROUGH) and 801464 (SPRINT). We also acknowledge support of the Base Funding – UIDB/00532/2020 and Programmatic Funding – UIDP/00532/2020 of the Transport Phenomena Research Centre – CEFT – funded by national funds through the FCT/MCTES (PIDDAC).

Competing interests

The authors have no competing interests to declare.

References

Akyol, Ş Melih, and Muhsin Kilic. 2010. "Dynamic Simulation of HVAC System Thermal Loads in an Automobile Compartment." *International Journal of Vehicle Design* 52 (1–4): 177–98. https://doi.org/10.1504/IJVD.2010.029643.

Alkan, Alpaslan, and Murat Hosoz. 2010. "Comparative Performance of an Automotive Air Conditioning System Using Fixed and Variable Capacity Compressors." *International Journal of Refrigeration* 33 (3): 487–95. https://doi.org/10.1016/j.ijrefrig.2009.12.018.

Andrew Pon Abraham, J. D., and M. Mohanraj. 2019. "Thermodynamic Performance of Automobile Air Conditioners Working with R430A as a Drop-in Substitute to R134a." *Journal of Thermal Analysis and Calorimetry* 136 (5): 2071–86. https://doi.org/10.1007/s10973-018-7843-1.

ASHRAE. 1997. "Chapter 8 - Thermal Comfort." In *1997 ASHRAE Handbook - Fundamentals*, edited by Robert A. Parsons, 8.12. Atlanta.

"Beja Air Base, Portugal - Weather Underground." n.d. Accessed September 28, 2018. https://www.wunderground.com/history/daily/po/beja/LPBJ/date/2018-7-21.

Boltzmann, Ludwig. 1884. "Ableitung Des Stefan'schen Gesetzes, Betreffend Die Abhängigkeit Der Wärmestrahlung von Der Temperatur Aus Der Electromagnetischen Lichttheorie." *Annalen Der Physik* 258 (6): 291–94. https://doi.org/10.1002/andp.18842580616.

Brotherhood, John R. 2008. "Heat Stress and Strain in Exercise and Sport." *Journal of*

Science and Medicine in Sport 11 (1): 6–19. https://doi.org/10.1016/j.jsams.2007.08.017.

Dadour, I R, I Almanjahie, N D Fowkes, G Keady, and K Vijayan. 2010. "Temperature Variations in a Parked Car." *Forensic Science International*.

"EnergyPlus - Evora, Portugal - Weather Data." n.d. Accessed September 28, 2018. https://energyplus.net/weather-location/europe_wmo_region_6/PRT//PRT_Evora.085570_IWEC.

Farrington, R, and J Rugh. 2000. "Impact of Vehicle Air-Conditioning on Fuel Economy, Tailpipe Emissions, and Electric Vehicle Range." In *Earth Technologies Forum*, http://www.nrel.gov/docs/fy00osti/28960.pdf. https://doi.org/NREL/CP-540-28960.

Farrington, Robert B, Deborah L Brodt, Steven D Burch, and Matthew a Keyser. 1998a. "Opportunities to Reduce Vehicle Climate Control Loads." In *Proceedings of the 15th Electric Vehicle Symposium*.

———. 1998b. "Opportunities to Reduce Vehicle Climate Control Loads." *Proceedings of the 15th Electric Vehicle Symposium*.

Fayazbakhsh, Mohammad Ali, and Majid Bahrami. 2013. "Comprehensive Modeling of Vehicle Air Conditioning Loads Using Heat Balance Method." In *SAE Technical Paper*. SAE International. https://doi.org/10.4271/2013-01-1507.

Flouris, Andreas D, Petros C Dinas, Leonidas G Ioannou, Lars Nybo, George Havenith, Glen P Kenny, and Tord Kjellstrom. 2018. "Workers' Health and Productivity under Occupational Heat Strain: A Systematic Review and Meta-Analysis." *The Lancet Planetary Health* 2 (12): e521–31. https://doi.org/10.1016/S2542-5196(18)30237-7.

Fontaras, Georgios, Theodoros Grigoratos, Dimitrios Savvidis, Konstantinos Anagnostopoulos, Raphael Luz, Martin Rexeis, and Stefan Hausberger. 2016. "An Experimental Evaluation of the Methodology Proposed for the Monitoring and Certification of CO2 Emissions from Heavy-Duty Vehicles in Europe." *Energy* 102 (May): 354–64. https://doi.org/10.1016/j.energy.2016.02.076.

Freund, Rudolf J., and William J. Wilson. 2003. *Statistical Methods - 2nd Edition*. Academic Press.

Fujita, Akihiro, Jun-ichi Kanemaru, Hiroshi Nakagawa, and Yoshiichi Ozeki. 2001. "Numerical Simulation Method to Predict the Thermal Environment inside a Car Cabin." *JSAE Review* 22.

Gravelle, Aled, Simon Robinson, and Alessandro Picarelli. 2015. "Modeling the Effects of Energy Efficient Glazing on Cabin Thermal Energy and Vehicle Efficiency." In *11th International Modelica Conference*, 291–300. https://doi.org/10.3384/ecp15118291.

Hajat, Shakoor, Madeline O'Connor, and Tom Kosatsky. 2010. "Health Effects of Hot Weather: From Awareness of Risk Factors to Effective Health Protection." *The Lancet* 375 (9717): 856–63. https://doi.org/10.1016/S0140-6736(09)61711-6.

Hanna, Elizabeth G., Tord Kjellstrom, Charmian Bennett, and Keith Dear. 2011. "Climate Change and Rising Heat: Population Health Implications for Working People in Australia." *Asia-Pacific Journal of Public Health* 23 (2 SUPPL.). https://doi.org/10.1177/1010539510391457.

Havenith, George, Ingvar Holmér, and Ken Parsons. 2002. "Personal Factors in Thermal Comfort Assessment: Clothing Properties and Metabolic Heat Production." *Energy and Buildings* 34 (6): 581–91. https://doi.org/10.1016/S0378-7788(02)00008-7.

Hodder, Simon G., and Ken Parsons. 2007. "The Effects of Solar Radiation on Thermal Comfort." *International Journal of Biometeorology* 51 (3): 233–50. https://doi.org/10.1007/s00484-006-0050-y.

Hoke, Paul B, and Christopher M Greiner. 2005. "Vehicle Paint Radiation Properties and Affect on Vehicle Soak Temperature, Climate Control System Load, and Fuel Economy." In *SAE Technical Paper*. SAE International. https://doi.org/10.4271/2005-01-1880.

Horak, Johannes, Ivo Schmerold, Kurt Wimmer, and Günther Schauberger. 2017. "Cabin Air Temperature of Parked Vehicles in Summer Conditions: Life-Threatening Environment for Children and Pets Calculated by a Dynamic Model." *Theoretical and Applied Climatology* 130: 107–18. https://doi.org/10.1007/s00704-016-1861-3.

Huang, Daniel, Michael Wallis, Emin Oker, and Steve Lepper. 2007. "Design of

Vehicle Air Conditioning Systems Using Heat Load Analysis." *SAE Technical Paper Series*, no. 724. https://doi.org/10.4271/2007-01-1196.

ISO 8996. 2004. *Ergonomics of the Thermal Environment — Determination of Metabolic Rate*. Geneva, Switzerland: International Organization for Standardization.

John, Prithiv, B Sriram, Senthil Kumar R, S Vinoth Kumar, Prakash Ramasamy, and C Vijay Ram. 2013. "Ventilation Improvement in a Non-AC Bus." In *SAE International*. https://doi.org/10.4271/2013-01-2457.

Joint Research Centre. 2016. *Report on VECTO Technology Simulation Capabilities and Future Outlook*. https://doi.org/10.2790/10868.

Khayyam, Hamid, Abbas Z. Kouzani, Eric J. Hu, and Saeid Nahavandi. 2011. "Coordinated Energy Management of Vehicle Air Conditioning System." *Applied Thermal Engineering* 31 (5): 750–64. https://doi.org/10.1016/j.applthermaleng.2010.10.022.

Kilic, Muhsin, and Gökhan Sevilgen. 2009. "Evaluation of Heat Transfer Characteristics in an Automobile Cabin with a Virtual Manikin During Heating Period." *Numerical Heat Transfer, Part A: Applications* 56 (6): 515–39. https://doi.org/10.1080/10407780903266356.

Klauer, Shelia G, Thomas A Dingus, Vicki L Neale, and Robert J Carroll. 2003. "The Effects of Fatigue on Driver Performance for Single and Team Long-Haul Truck Drivers." In *Driving Assessment Conference*, 143–47. https://doi.org/10.17077/drivingassessment.1109.

Kopfer, Heiko W, and Udo Buscher. 2015. "A Comparison of the Productivity of Single Manning and Multi Manning for Road Transportation Tasks." In *Logistics Management*, edited by Jan Dethloff, Hans-Dietrich Haasis, Herbert Kopfer, Herbert Kotzab, and Jörn Schönberger, 277–87. Cham: Springer International Publishing.

Lahimer, A. A., M. A. Alghoul, K. Sopian, and N. G. Khrit. 2018. "Potential of Solar Reflective Cover on Regulating the Car Cabin Conditions and Fuel Consumption." *Applied Thermal Engineering* 143 (April): 59–71. https://doi.org/10.1016/j.applthermaleng.2018.07.020.

Levinson, Ronnen, Hashem Akbari, George Ban-Weiss, Heng Pan, Riccardo Paolini, Pablo Rosado, Michael Spears, and Joyce Tam. 2010. “Cool-colored Cars to Reduce Air-conditioning Energy Use and Reduce CO2 Emission.”

Levinson, Ronnen, Heng Pan, George Ban-Weiss, Pablo Rosado, Riccardo Paolini, and Hashem Akbari. 2011. “Potential Benefits of Solar Reflective Car Shells: Cooler Cabins, Fuel Savings and Emission Reductions.” *Applied Energy* 88 (12): 4343–57. https://doi.org/10.1016/j.apenergy.2011.05.006.

Li, Wenhua, and Jian Sun. 2013. “Numerical Simulation and Analysis of Transport Air Conditioning System Integrated with Passenger Compartment.” *Applied Thermal Engineering* 50 (1): 37–45. https://doi.org/10.1016/j.applthermaleng.2012.05.030.

Mallick, P.K. 2012. “Advanced Materials for Automotive Applications: An Overview.” In *Advanced Materials in Automotive Engineering*, edited by Jason Rowe, 5–27. Elsevier. https://doi.org/10.1533/9780857095466.5.

MAN. n.d. “TGX Design & Cabs.” Accessed March 28, 2019. https://www.truck.man.eu/uk/en/trucks/tgx/overview/tgx.html#design__cabs.

Marcos, David, Francisco J. Pino, Carlos Bordons, and José J. Guerra. 2014. “The Development and Validation of a Thermal Model for the Cabin of a Vehicle.” *Applied Thermal Engineering* 66 (1–2): 646–56. https://doi.org/10.1016/j.applthermaleng.2014.02.054.

Martini, Helena, Peter Gullberg, and Lennart Lofdahl. 2018. “Aerodynamic Analysis of Cooling Airflow for Different Front-End Designs of a Heavy-Duty Cab-Over-Engine Truck.” *SAE International Journal of Commercial Vehicles* 11 (1): 31–44. https://doi.org/10.4271/02-11-01-0003.

Mercedes Benz. n.d. “Actros Cab Variants.” Accessed March 28, 2019. https://www.mercedes-benz-trucks.com/en_GB/models/new-actros/technical-data/cab-variants.html.

Mezrhab, A, and M Bouzidi. 2006. “Computation of Thermal Comfort inside a Passenger Car Compartment.” *Applied Thermal Engineering* 26: 1697–1704. https://doi.org/10.1016/j.applthermaleng.2005.11.008.

Morello, Lorenzo, Lorenzo Rossini, Pia Giuseppe, and Andrea Tonoli. 2011. *The Automotive Body Volume I: Components Design*. *Springer*.

https://doi.org/10.1007/978-94-007-0513-5_6.

Muncrief, Rachel, and Ben Sharpe. 2015. "Overview of the Heavy-Duty Vehicle Market and CO2 Emissions in the European Union." *International Council on Clean Transportation*. https://doi.org/10.1007/978-3-319-76451-1_34.

Musat, Radu, and Elena Helerea. 2009. "Parameters and Models of the Vehicle Thermal Comfort." *Electrical and Mechanical Engineering* 1: 215–26. http://www.acta.sapientia.ro/acta-emeng/C1/emeng1-19.pdf.

Na, Kwangsam, Subhasis Biswas, William Robertson, Keshav Sahay, Robert Okamoto, Alexander Mitchell, and Sharon Lemieux. 2015. "Impact of Biodiesel and Renewable Diesel on Emissions of Regulated Pollutants and Greenhouse Gases on a 2000 Heavy Duty Diesel Truck." *Atmospheric Environment* 107 (x): 307–14. https://doi.org/10.1016/j.atmosenv.2015.02.054.

"National Oceanic and Atmospheric Administration." 2021. U.S. Department of Commerce. 2021.

Olson, Kurt, Steven Adelman, Cory Kreutzer, James Ohlinger, Jason Aaron Lustbader, Skip Yeakel, Philip Brontz, and Matthew A. Jeffers. 2014. "Impact of Paint Color on Rest Period Climate Control Loads in Long-Haul Trucks." *SAE Technical Paper Series* 1. https://doi.org/10.4271/2014-01-0680.

Orzechowski, T., and Z. Skrobacki. 2016. "Evaluation of Thermal Conditions inside a Vehicle Cabin." *EPJ Web of Conferences* 114: 1–5. https://doi.org/10.1051/epjconf/201611402085.

Parsons, Ken. 2003. "Human Thermal Physiology and Thermoregulation." In *Human Thermal Environments: The Effects of Hot, Moderate, and Cold Environments on Human Health, Comfort and Performance*, 29–46. London: Taylor & Francis.

Pokorny, Jan, Jan Fiser, and Miroslav Jicha. 2014. "A Parametric Study of Influence of Material Properties on Car Cabin Environment." In *EPJ Web of Conferences*, 67:2–5. https://doi.org/10.1051/epjconf/20146702096.

Poulianiti, Konstantina P., George Havenith, and Andreas D. Flouris. 2018. "Metabolic Energy Cost of Workers in Agriculture, Construction, Manufacturing, Tourism, and Transportation Industries." *Industrial Health*. https://doi.org/10.2486/indhealth.2018-0075.

Qi, Zhaogang, Yu Zhao, and Jiangping Chen. 2010. “Performance Enhancement Study of Mobile Air Conditioning System Using Microchannel Heat Exchangers.” *International Journal of Refrigeration* 33 (2): 301–12. https://doi.org/10.1016/j.ijrefrig.2009.08.014.

Rexeis, Martin, Martin Röck, Markus Quaritsch, Stefan Hausberger, and Gérard Silberholz. 2019. “Further Development of VECTO.”

Rugh, John. 2009. “Impact of Sungate EP on PHEV Performance - Results of a Simulated Solar Reflective Glass PHEV Dynamometer Test.”

Rugh, John P, Lawrence Chaney, Jason Lustbader, and John Meyer. 2007. “Reduction in Vehicle Temperatures and Fuel Use from Cabin Ventilation, Solar-Reflective Paint, and a New Solar-Reflective Glazing.” In *SAE Technical Papers*. https://doi.org/10.4271/2007-01-1194.

Rugh, John P, Terry J Hendricks, and Kwaku Koram. 2001. “Effect of Solar Reflective Glazing on Ford Explorer Climate Control, Fuel Economy, and Emissions.” In *SAE Technical Paper Series*. https://doi.org/10.4271/2001-01-3077.

Saari, Sampo, Panu Karjalainen, Leonidas Ntziachristos, Liisa Pirjola, Pekka Matilainen, Jorma Keskinen, and Topi Rönkkö. 2016. “Exhaust Particle and NOx Emission Performance of an SCR Heavy Duty Truck Operating in Real-World Conditions.” *Atmospheric Environment* 126 (2): 136–44. https://doi.org/10.1016/j.atmosenv.2015.11.047.

Samuel, S., L. Austin, and D. Morrey. 2002. “Automotive Test Drive Cycles for Emission Measurement and Real-World Emission Levels-a Review.” *Proceedings of the Institution of Mechanical Engineers, Part D: Journal of Automobile Engineering* 216 (7): 555–64. https://doi.org/10.1243/095440702760178587.

Swinbank, W. C. 1963. “Long-Wave Radiation from Clear Skies.” *Quarterly Journal of the Royal Meteorological Society* 89 (381): 339–48. https://doi.org/10.1002/qj.49708938105.

Tansini, Alessandro, Georgios Fontaras, Biagio Ciuffo, Federico Millo, Iker Prado Rujas, and Nikiforos Zacharof. 2019. “Calculating Heavy-Duty Truck Energy and Fuel Consumption Using Correlation Formulas Derived from Vecto Simulations.” *SAE Technical Papers* 2019-April (April): 1–21. https://doi.org/10.4271/2019-01-

1278.

Torregrosa-Jaime, Bárbara, Filip Bjurling, José M. Corberán, Fausto Di Sciullo, and Jorge Payá. 2015. “Transient Thermal Model of a Vehicle’s Cabin Validated under Variable Ambient Conditions.” *Applied Thermal Engineering* 75: 45–53. https://doi.org/10.1016/j.applthermaleng.2014.05.074.

Vale, João P., Pedro G. Alves, and Tiago S. Mayor. 2020. “Supplementary Data for Heavy Duty Truck Thermal Modelling.” https://doi.org/10.6084/m9.figshare.12514031.

Venugopal, Vidhya, Jeremiah S. Chinnadurai, Rebekah A.I. Lucas, and Tord Kjellstrom. 2015. “Occupational Heat Stress Profiles in Selected Workplaces in India.” *International Journal of Environmental Research and Public Health* 13 (1): 1–13. https://doi.org/10.3390/ijerph13010089.

Volvo. n.d. “Cab Specifications.” https://www.volvotrucks.com/en-sy/trucks/volvo-fh-series/specifications/cab.html.

———. 2018. “Fuel Consumption.” 2018.

Walgama, C., S. Fackrell, M. Karimi, A. Fartaj, and G. W. Rankin. 2006. “Passenger Thermal Comfort in Vehicles - A Review.” *Proceedings of the Institution of Mechanical Engineers, Part D: Journal of Automobile Engineering* 220 (5): 543–62. https://doi.org/10.1243/09544070D00705.

Watts, Nick, W. Neil Adger, Paolo Agnolucci, Jason Blackstock, Peter Byass, Wenjia Cai, Sarah Chaytor, et al. 2015. “Health and Climate Change: Policy Responses to Protect Public Health.” *The Lancet* 386 (10006): 1861–1914. https://doi.org/10.1016/S0140-6736(15)60854-6.

Wong, L.T., and W.K. Chow. 2001. “Solar Radiation Model.” *Applied Energy* 69 (3): 191–224. https://doi.org/10.1016/S0306-2619(01)00012-5.

Zacharof, Nikiforos, Orkun Özener, Muammer Özkan, Abdullah Kilicaslan, and Georgios Fontaras. 2019. “Simulating City-Bus On-Road Operation With VECTO.” *Frontiers in Mechanical Engineering* 5 (September). https://doi.org/10.3389/fmech.2019.00058.

Zheng, Yinhua, Brown Mark, and Harry Youmans. 2011. “A Simple Method to Calculate Vehicle Heat Load.” In *SAE Technical Paper*. Vol. 2011-01–01.

https://doi.org/10.4271/2011-01-0127.

Table 1 – Properties of the truck surfaces considered in this study: area (A_s), thickness (δ_s), density (ρ_s), specific heat (c_s), conductivity (k_s), absorptivity (α_s), transmissivity (τ_s) and emissivity (ε_s).

Surface	A_s $[m^2]$	δ_s $[m]$	ρ_s $[kg \cdot m^{-3}]$	c_s $[J \cdot kg^{-1}K^{-1}]$	k_s $[W \cdot m^{-1}K^{-1}]$	α_s $[-]$	τ_s $[-]$	ε_s $[-]$
Front	2.625	0.012	775	600	0.041	0.68	0.00	0.90
Windshield	1.575	0.003	2500	840	1.05	0.45	0.50	0.95
Left Window	0.56	0.003	2500	840	1.05	0.46	0.49	0.95
Left Door	3.44	0.012	775	600	0.041	0.68	0.00	0.90
Right Window	0.56	0.003	2500	840	1.05	0.46	0.49	0.95
Right Door	3.44	0.012	775	600	0.041	0.68	0.00	0.90
Back	4.2	0.012	775	600	0.041	0.68	0.00	0.90
Roof	4.2	0.012	775	600	0.041	0.68	0.00	0.90
Base	4.2	0.012	775	600	0.041	0.68	0.00	0.90

Table 2 – Data for the virtual subjects inside the cabin. M is the metabolic heat production rate (estimated based on ISO 8996:2004 (ISO 8996 2004) and Poulianiti et al. (Poulianiti, Havenith, and Flouris 2018))

Variables	Driver	Passenger
Height [m]	1.7	1.6
Weight [kg]	70	60
M [W/m^2]	85	55

Table 3 – Constants required to estimate the solar radiation load for July (ASHRAE 1997)

A	B	C
1084.88	0.207	0.136

Table 4 - Optical properties of the different scenarios for the cabin windshield, side windows and external paint. White cells indicate that the properties are the standard for a truck. Red indicates the properties increase heat loads on the cabin, whereas green indicates the properties decrease heat loads on the cabin.

	Windshield				Side Windows				Paint			
Scenarios	transmissivity (τ)	absorptivity (α)	reflectivity (ρ)	emissivity (ε)	transmissivity (τ)	absorptivity (α)	reflectivity (ρ)	emissivity (ε)	transmissivity (τ)	absorptivity (α)	reflectivity (ρ)	emissivity (ε)
1-STANDARD	0.50	0.45	0.05	0.95	0.49	0.46	0.05	0.95	0	0.68	0.32	0.90
2-HIGH-TRANSMISSIVITY GLAZING	0.79	0.14	0.07	0.95	0.84	0.08	0.08	0.95	0	0.68	0.32	0.90
3-LOW-TRANSMISSIVITY GLAZING	0.33	0.20	0.47	0.95	0.33	0.20	0.47	0.95	0	0.68	0.32	0.90
4-LOW-REFLECTIVITY PAINT	0.50	0.45	0.05	0.95	0.49	0.46	0.05	0.95	0	0.96	0.04	0.89
5-HIGH-REFLECTIVITY PAINT	0.50	0.45	0.05	0.95	0.49	0.46	0.05	0.95	0	0.30	0.70	0.88
6-HIGH-TRANS. GLAZING & LOW-REFL. PAINT	0.79	0.14	0.07	0.95	0.84	0.08	0.08	0.95	0	0.96	0.04	0.89
7-LOW-TRANS. GLAZING & HIGH-REFL. PAINT	0.33	0.20	0.47	0.95	0.33	0.20	0.47	0.95	0	0.30	0.70	0.88

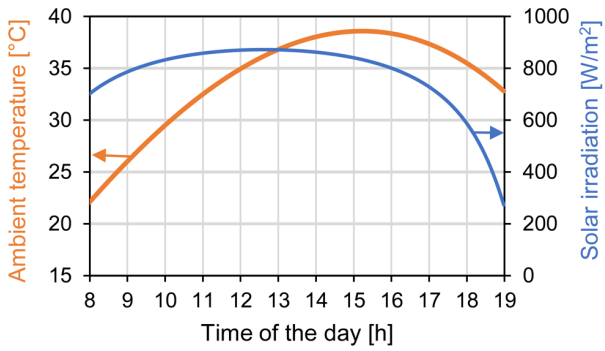

Figure 1 – Variation of the ambient air temperature (T_{amb}) and solar irradiance (I_{dir}) over time in Évora, Portugal during a summer workday (21st of July).

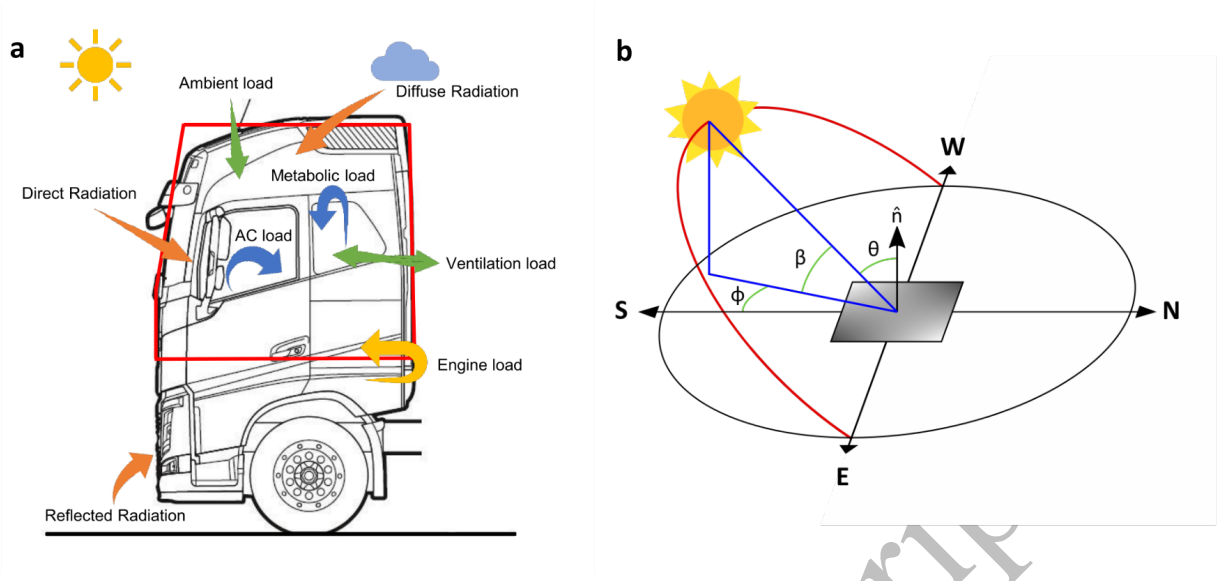

Figure 2 – (a) Loads that affect a vehicle cabin exposed to the surrounding environment (adapted from the Volvo cab specifications (Volvo, n.d.)) and (b) Angles of the sun in relation to a surface with normal vector n̂. β is the altitude angle, ϕ is the azimuth angle and θ is the angle between the surface normal and the position vector of the sun.

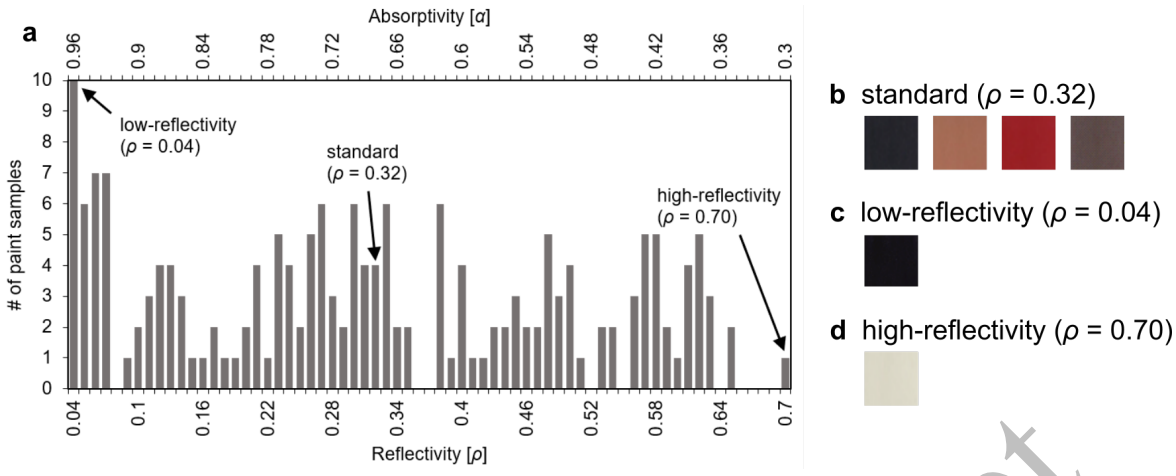

Figure 3 - (a) Histogram of reflectivity values (ρ) from the paints in the "CoolCars" database (Levinson et al. 2010); Examples of paint colours considered as (b) Standard paint (refs: CBASF047, CPPG040, CBASF042 and CBASF045, ρ = 0.32); (c) Low-reflectivity paint (ref: CBASF026, ρ = 0.04) and (d) High-reflectivity paint (ref: CBASF063, ρ = 0.70); The reflectivity of the standard, low-reflectivity and high-reflectivity paints corresponds to the average, minimum and maximum reflectivity of the paints in the database.

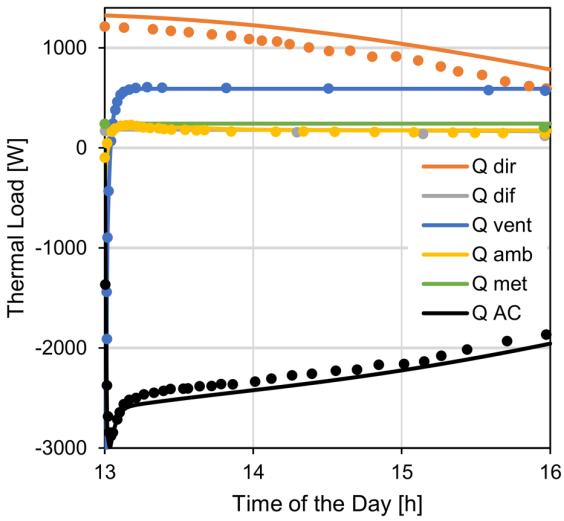

Figure 4 – Thermal loads obtained by Fayazbakhsh and Bahrami (Fayazbakhsh and Bahrami 2013) (circles) and by the present model (lines), for the conditions reported in the mentioned study.

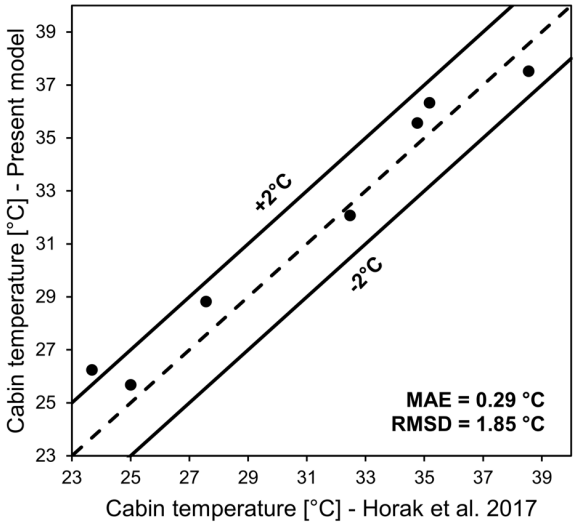

Figure 5 – Comparison of experimental (x axis, Horak et al. (Horak et al. 2017)) and predicted (y axis, present model) cabin temperatures , after 1 h exposures for various environmental conditions. Dashed line represents the identity line and the two full lines mark the +/- 2 °C region around the identity line. MAE and RMSD stand for mean absolute error and root-mean-squared deviation, respectively.

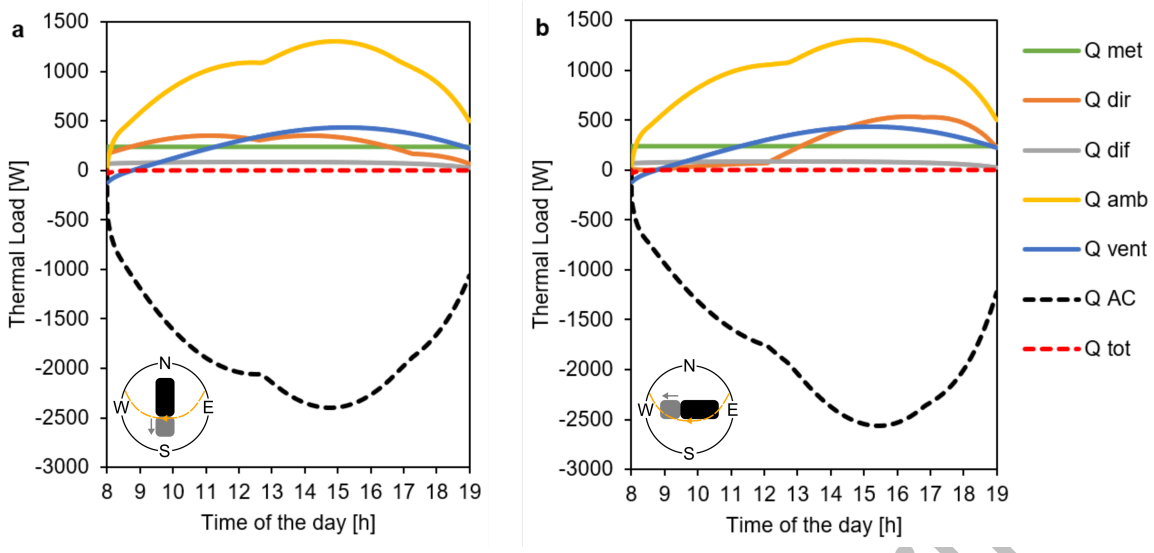

Figure 6 – Thermal loads during a day for trucks driving (a) south and (b) west. The plots on the top right corner of each panel are the representation of the truck directions considered in the simulations relative to the position/motion of the sun (heading south and west respectively). The sketch on the left bottom corner of the charts shows the approximate solar movement during the day (yellow line) relative to the truck direction (grey arrow).

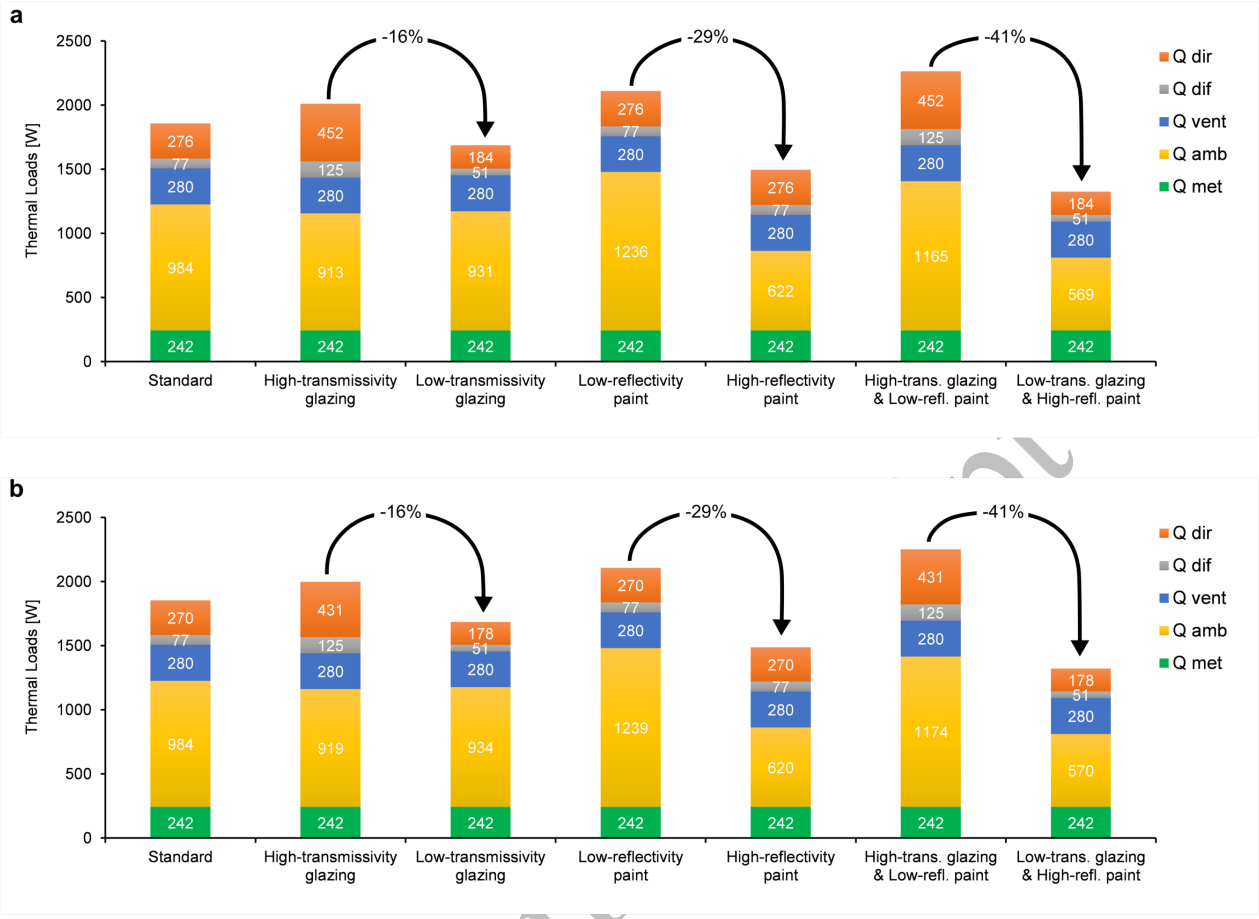

Figure 7 – Daily average thermal loads for trucks moving south (a) and west (b), for the different scenarios considered (Table 4), regarding the transmissivity and reflectivity of the cabin glazing or external paint. The different thermal loads (Q dir, Q dif, Q vent, Q amb and Q met) are stacked in bars for each of the scenarios that were considered and their respective values are labeled inside the bars. The sum of these thermal loads yields the AC cooling load (equation 17) and the change in AC cooling load between different scenarios is represented by the arrows.

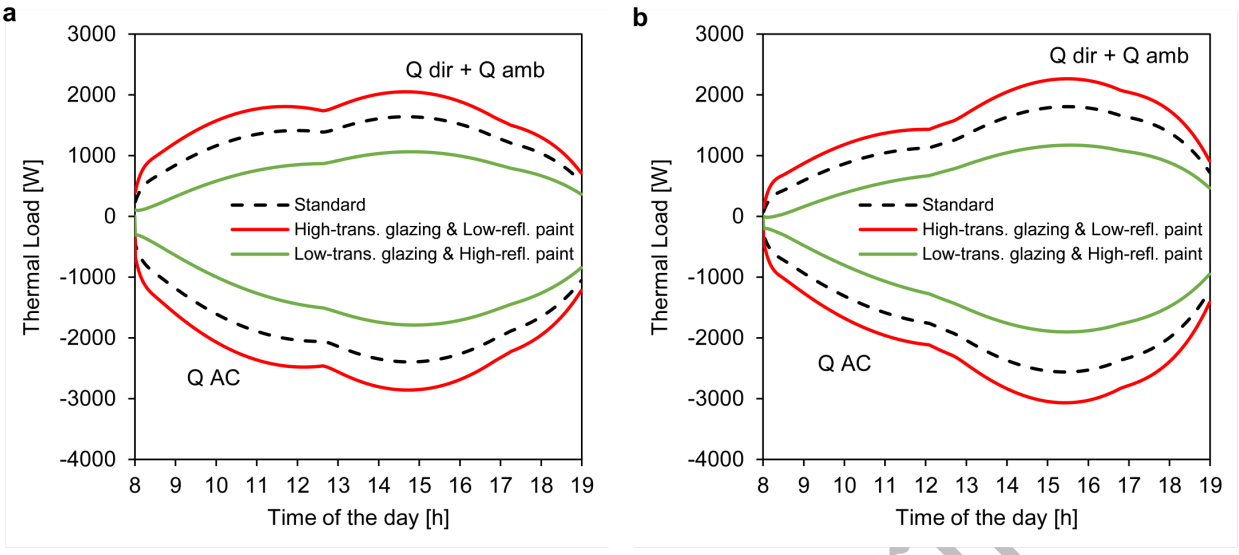

Figure 8 – Cooling load (Q AC) and sum of the direct radiation and ambient loads (Q dir + Q amb) throughout the day for trucks heading south (a) and west (b). Results for trucks with standard, high-transmissivity glazing & low-reflectivity paint, and low-transmissivity glazing & high-reflectivity paint configurations (scenarios 1, 6 and 7 respectively, Table 4); positive or negative loads imply heat entering or exiting the cabin, respectively.

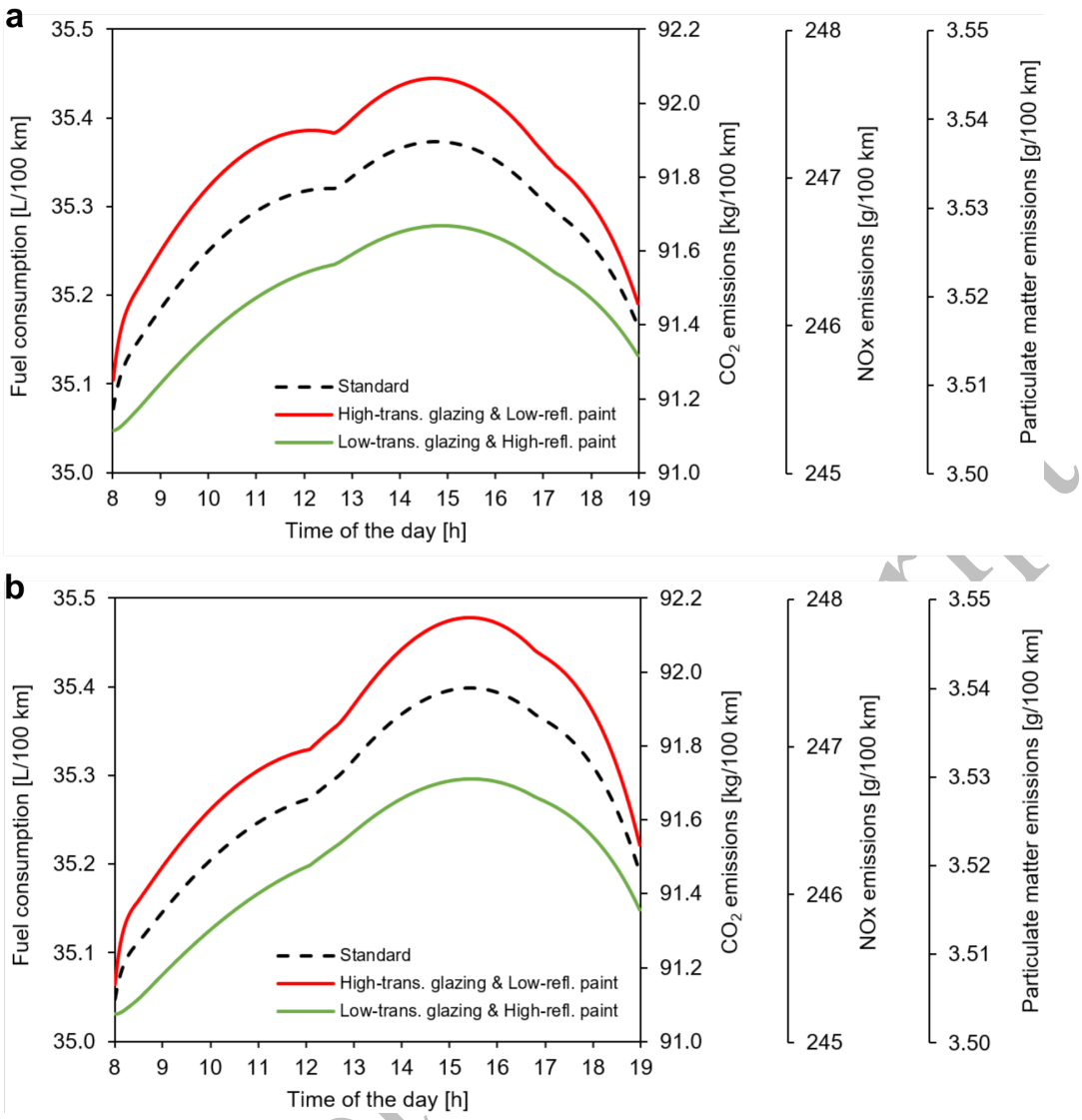

Figure 9 – Fuel consumption and CO_2, NO_x, and particulate matter emissions throughout the day for trucks heading (a) south and (b) west. Results for trucks with standard, high-transmissivity glazing & low-reflectivity paint, and low-transmissivity glazing & high-reflectivity paint configurations (scenarios 1, 6 and 7 respectively, Table 4). Due to the linear relation between fuel consumption and emissions, the curves for fuel consumption and (CO_2, NO_x and particulate) emissions are similar, but should be read in the respective y-axis.

Figure 1 – Variation of the ambient air temperature (T_{amb}) and solar irradiance (I_{dir}) over time in Évora, Portugal during a summer workday (21st of July).

Figure 2 – (a) Loads that affect a vehicle cabin exposed to the surrounding environment (adapted from the Volvo cab specifications (Volvo, n.d.)) and (b) Angles of the sun in relation to a surface with normal vector n̂. β is the altitude angle, ϕ is the azimuth angle and θ is the angle between the surface normal and the position vector of the sun.

Figure 3 - (a) Histogram of reflectivity values (ρ) from the paints in the "CoolCars" database (Levinson et al. 2010); Examples of paint colours considered as (b) Standard paint (refs: CBASF047, CPPG040, CBASF042 and CBASF045, ρ = 0.32); (c) Low-reflectivity paint (ref: CBASF026, ρ = 0.04) and (d) High-reflectivity paint (ref: CBASF063, ρ = 0.70); The reflectivity of the standard, low-reflectivity and high-reflectivity paints corresponds to the average, minimum and maximum reflectivity of the paints in the database.

Figure 4 – Thermal loads obtained by Fayazbakhsh and Bahrami (Fayazbakhsh and Bahrami 2013) (circles) and by the present model (lines), for the conditions reported in the mentioned study.

Figure 5 – Comparison of experimental (x axis, Horak et al. (Horak et al. 2017)) and predicted (y axis, present model) cabin temperatures , after 1 h exposures for various environmental conditions. Dashed line represents the identity line and the two full lines mark the +/- 2 °C region around the identity line. MAE and RMSD stand for mean absolute error and root-mean-squared deviation, respectively.

Figure 6 – Thermal loads during a day for trucks driving (a) south and (b) west. The plots on the top right corner of each panel are the representation of the truck directions considered in the simulations relative to the position/motion of the sun (heading south and west respectively). The sketch on the left bottom corner of the charts shows the approximate solar movement during the day (yellow line) relative to the truck direction (grey arrow).

Figure 7 – Daily average thermal loads for trucks moving south (a) and west (b), for the different scenarios considered (Table 4), regarding the transmissivity and reflectivity of the cabin glazing or external paint. The different thermal loads (Q dir, Q dif, Q vent, Q

amb and Q met) are stacked in bars for each of the scenarios that were considered and their respective values are labeled inside the bars. The sum of these thermal loads yields the AC cooling load (equation 17) and the change in AC cooling load between different scenarios is represented by the arrows.

Figure 8 – Cooling load (Q AC) and sum of the direct radiation and ambient loads (Q dir + Q amb) throughout the day for trucks heading south (a) and west (b). Results for trucks with standard, high-transmissivity glazing & low-reflectivity paint, and low-transmissivity glazing & high-reflectivity paint configurations (scenarios 1, 6 and 7 respectively, Table 4); positive or negative loads imply heat entering or exiting the cabin, respectively.

Figure 9 – Fuel consumption and CO2, NOx, and particulate matter emissions throughout the day for trucks heading (a) south and (b) west. Results for trucks with standard, high-transmissivity glazing & low-reflectivity paint, and low-transmissivity glazing & high-reflectivity paint configurations (scenarios 1, 6 and 7 respectively, Table 4). Due to the linear relation between fuel consumption and emissions, the curves for fuel consumption and (CO2, NOx and particulate) emissions are similar, but should be read in the respective y-axis.